Supporting Information for

Synthesis and Structure of Dinuclear Cationic Aluminum Complexes

Xinbgao Wang, Vincent Dorcet, Yi Luo, Jean-Francois Carpentier and Evgueni Kirillov

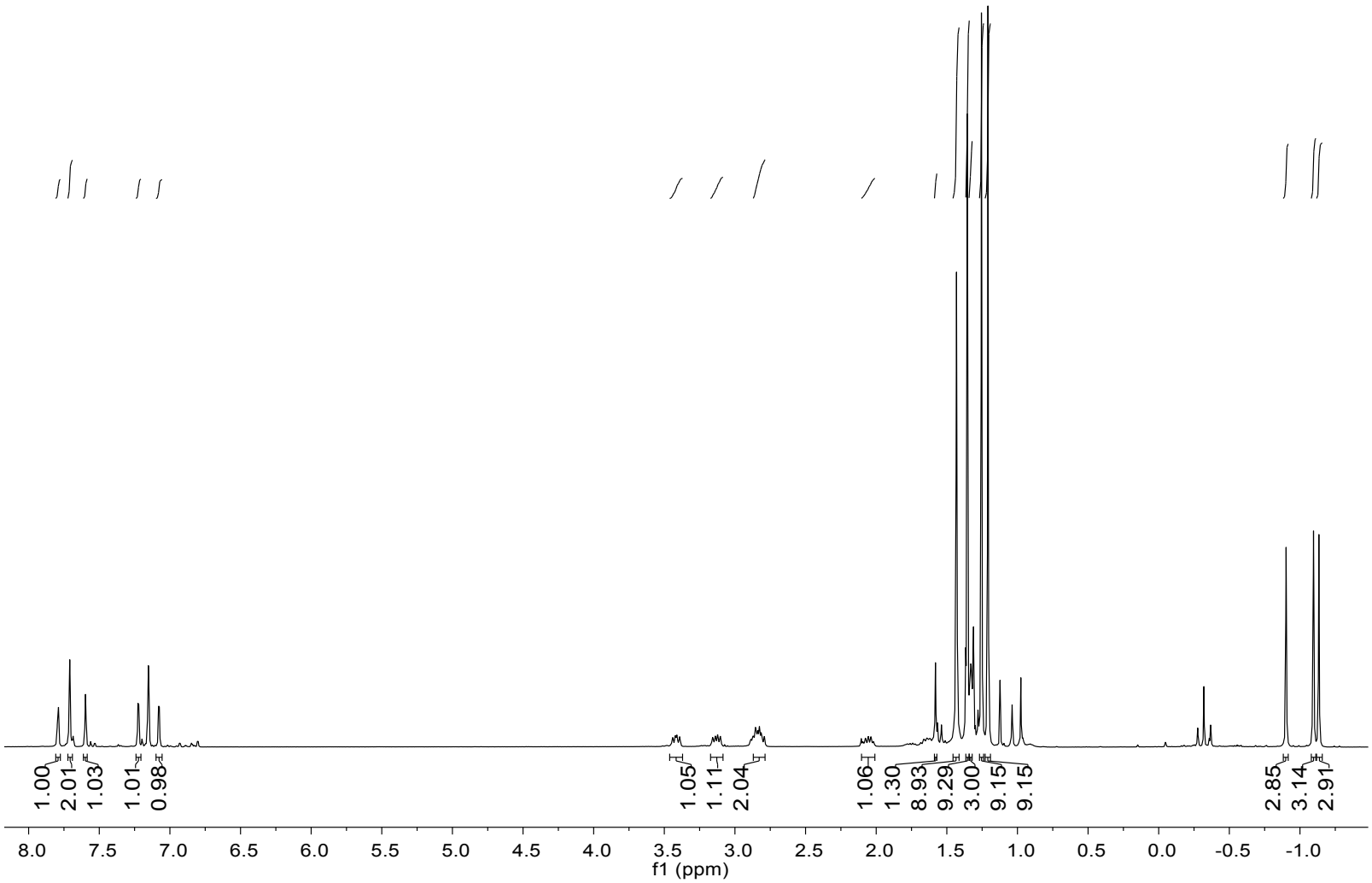

Figure S1. ^{1}H NMR spectrum (400 MHz, C_6D_6, 298 K) of **[2a]$^{+}$[MeB(C$_6$F$_5$)$_3$]$^{-}$**.

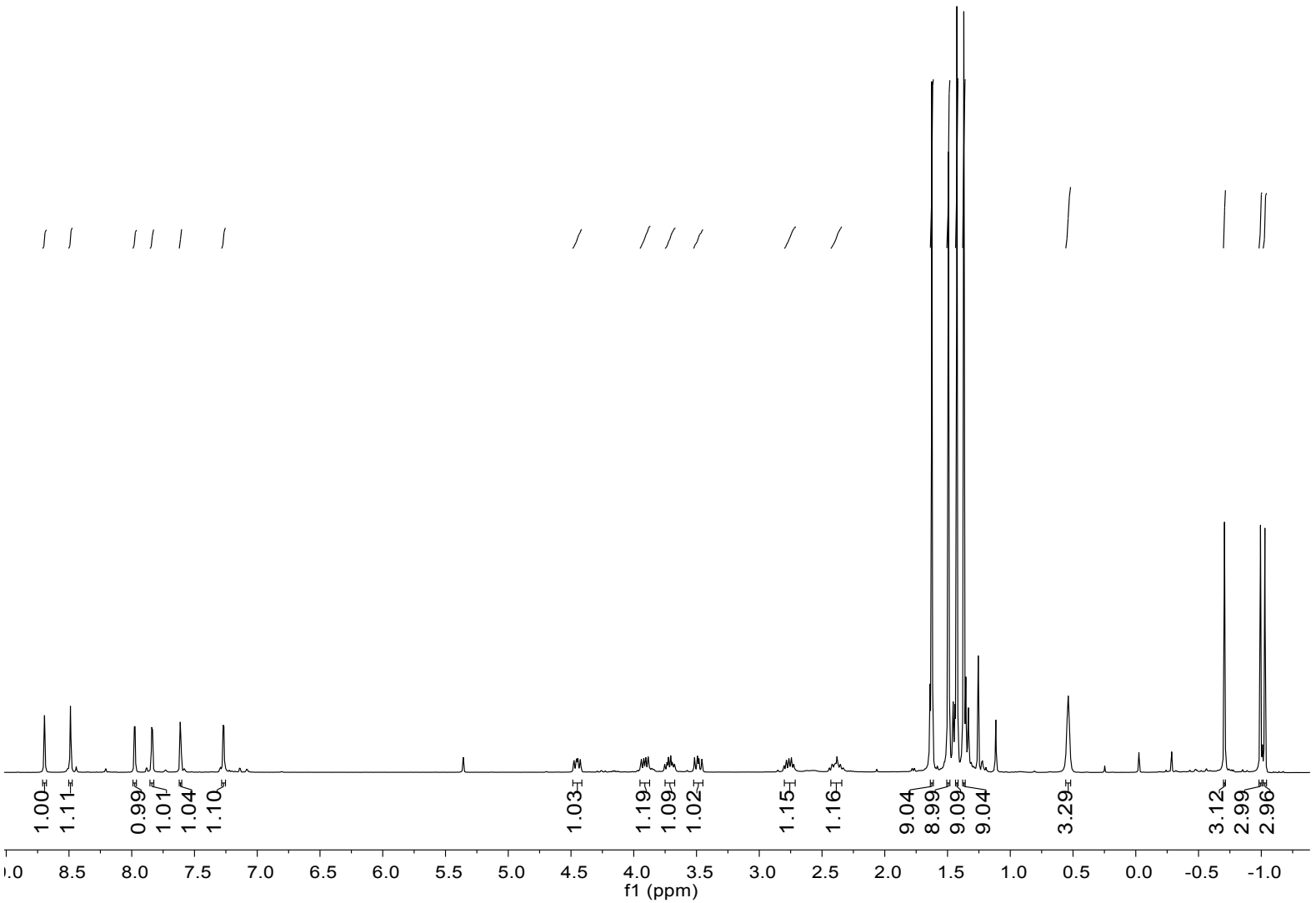

Figure S2. ^{1}H NMR spectrum (400 MHz, CD_2Cl_2, 298 K) of **[2a]$^{+}$[MeB(C_6F_5)$_3$]$^{-}$**.

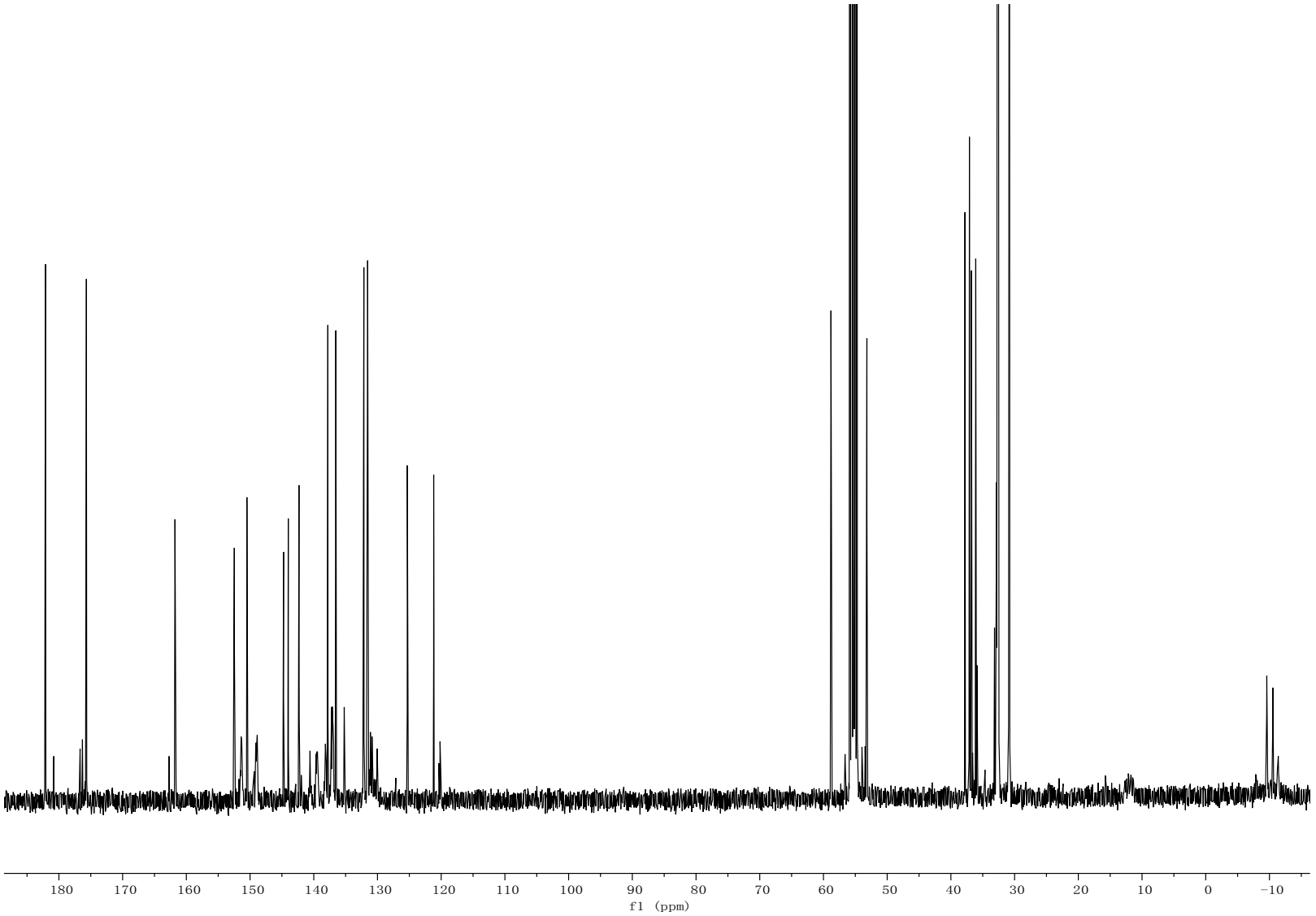

Figure S3. $^{13}C\{^{1}H\}$ NMR spectrum (100 MHz, CD_2Cl_2, 298 K) of **[2a]$^{+}$[MeB(C_6F_5)$_3$]$^{-}$**.

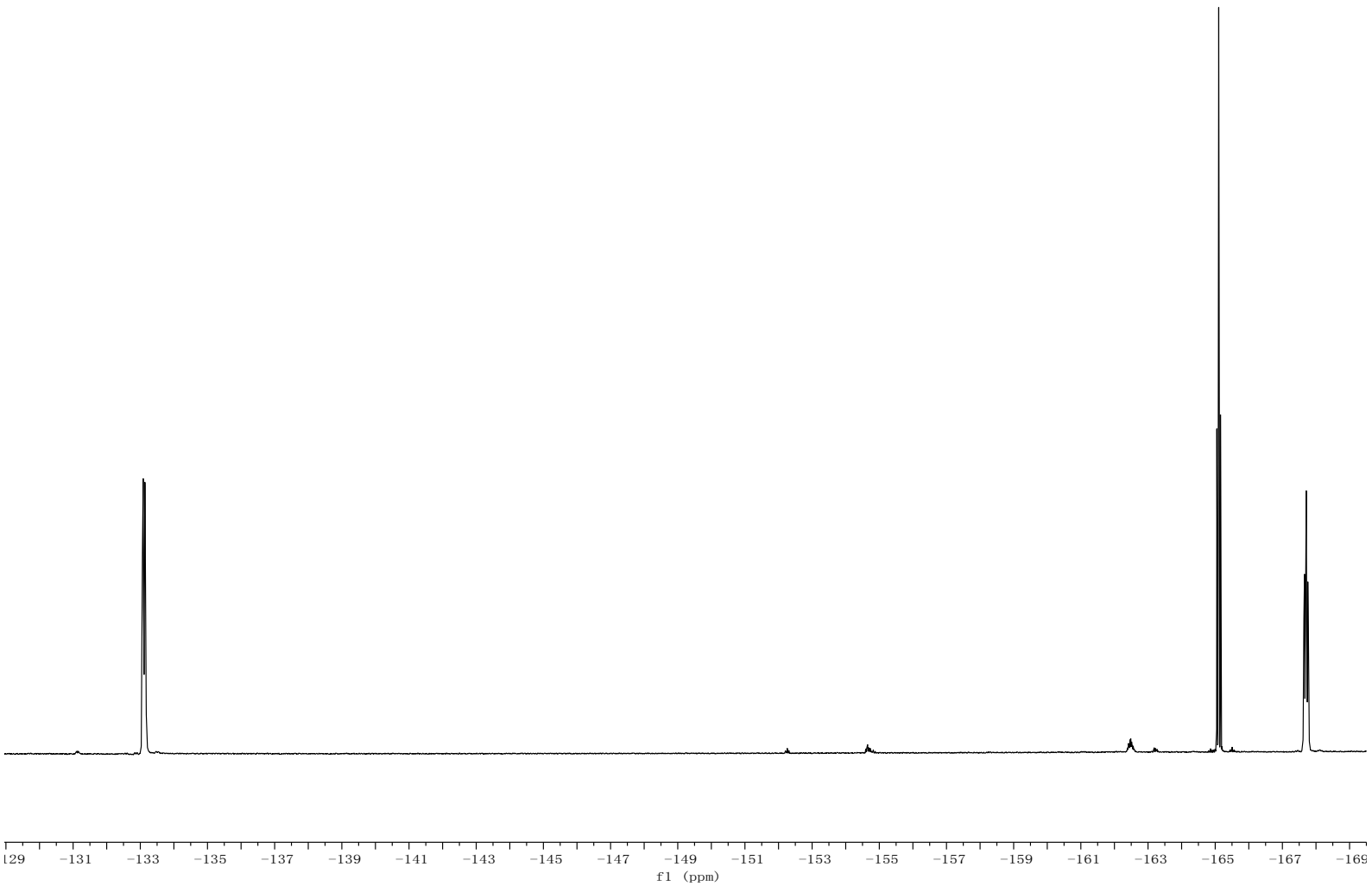

Figure S4. $^{19}F\{^{1}H\}$ NMR spectrum (376 MHz, CD_2Cl_2, 298 K) of **[2a]$^+$[MeB(C_6F_5)$_3$]$^-$**.

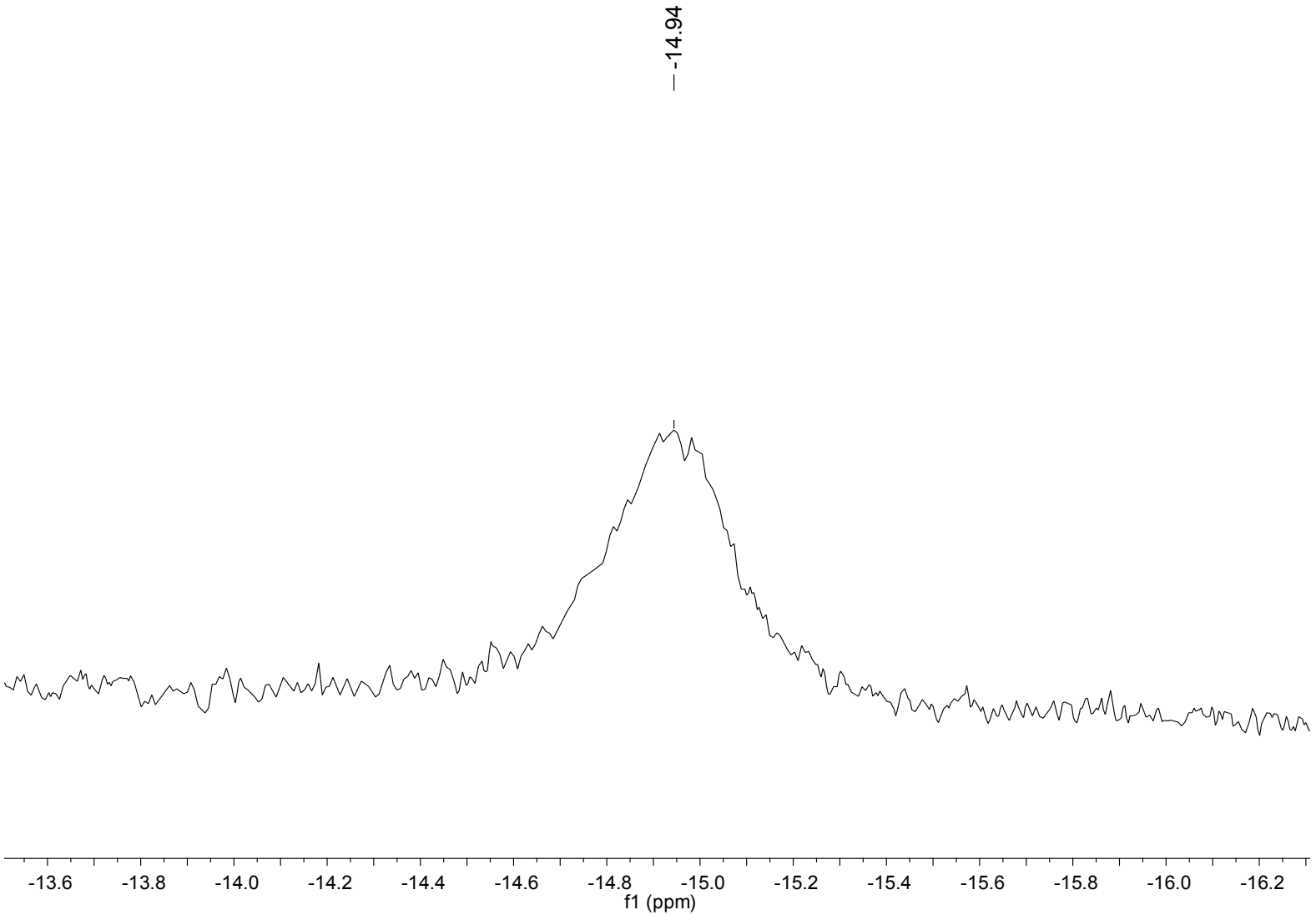

Figure S5. $^{11}B\{^{1}H\}$ NMR spectrum (128 MHz, CD_2Cl_2, 298 K) of **[2a]$^{+}$[MeB(C_6F_5)$_3$]$^{-}$**.

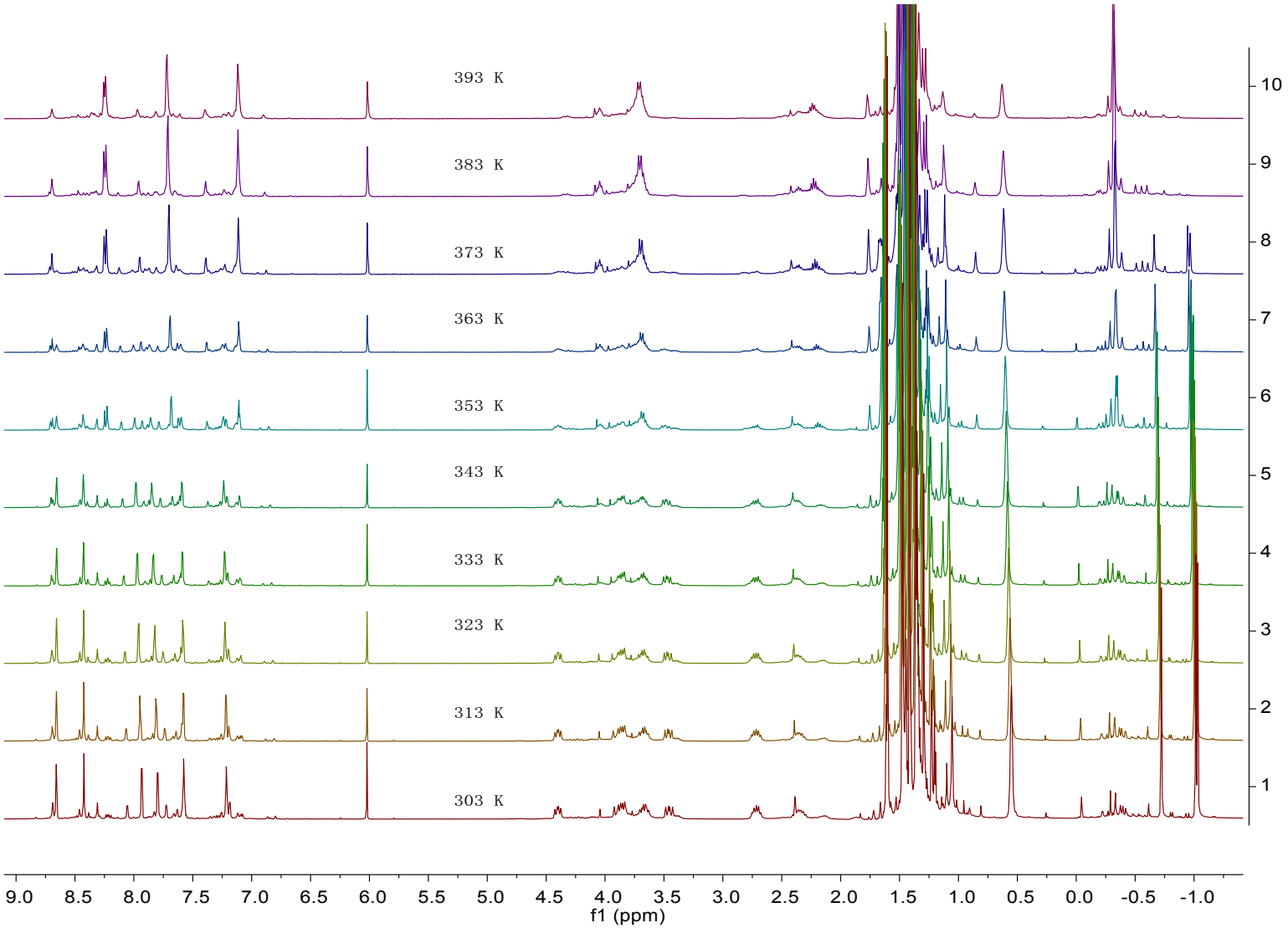

Figure S6. Variable-temperature ^{1}H NMR spectrum (400 MHz, $C_2D_2Cl_4$) of **[2a]$^{+}$[MeB(C$_6$F$_5$)$_3$]$^{-}$**.

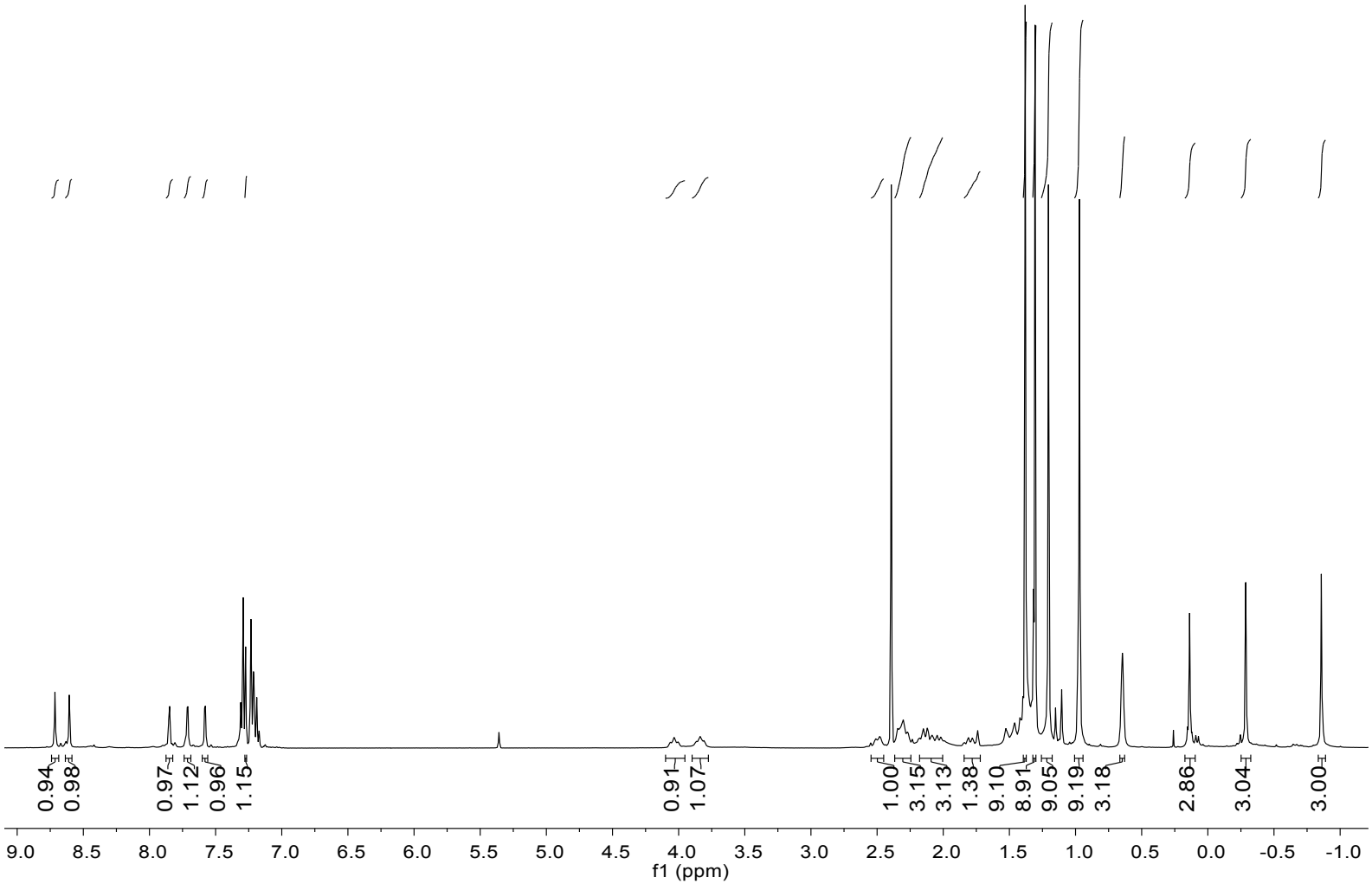

Figure S7. ^{1}H NMR spectrum (400 MHz, CD_2Cl_2, 298 K) of **[2b]$^{+}$[MeB(C_6F_5)$_3$]$^{-}$**.

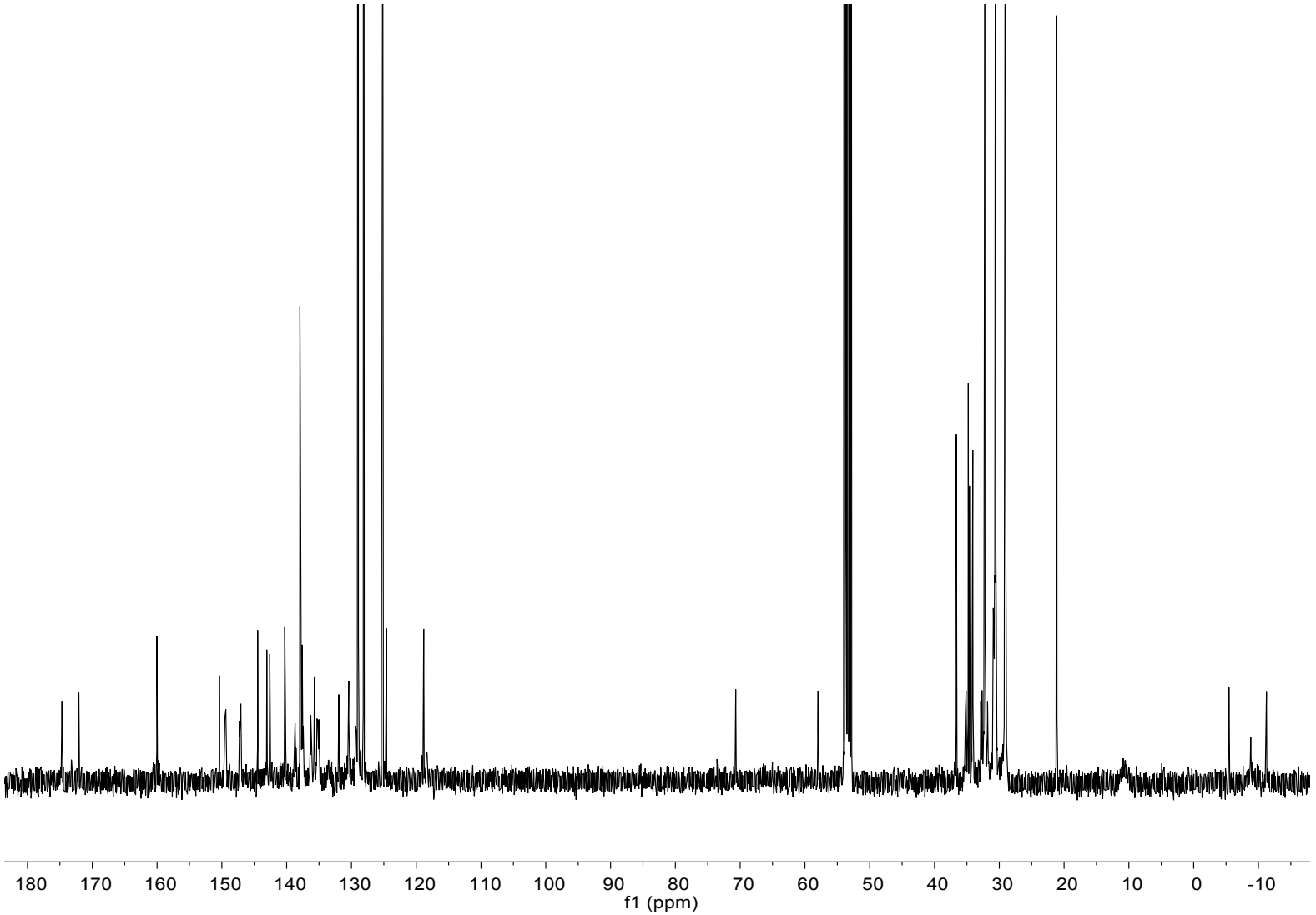

Figure S8. $^{13}C\{^{1}H\}$ NMR spectrum (100 MHz, CD_2Cl_2, 298 K) of **[2b]$^{+}$[MeB(C$_6$F$_5$)$_3$]$^{-}$**.

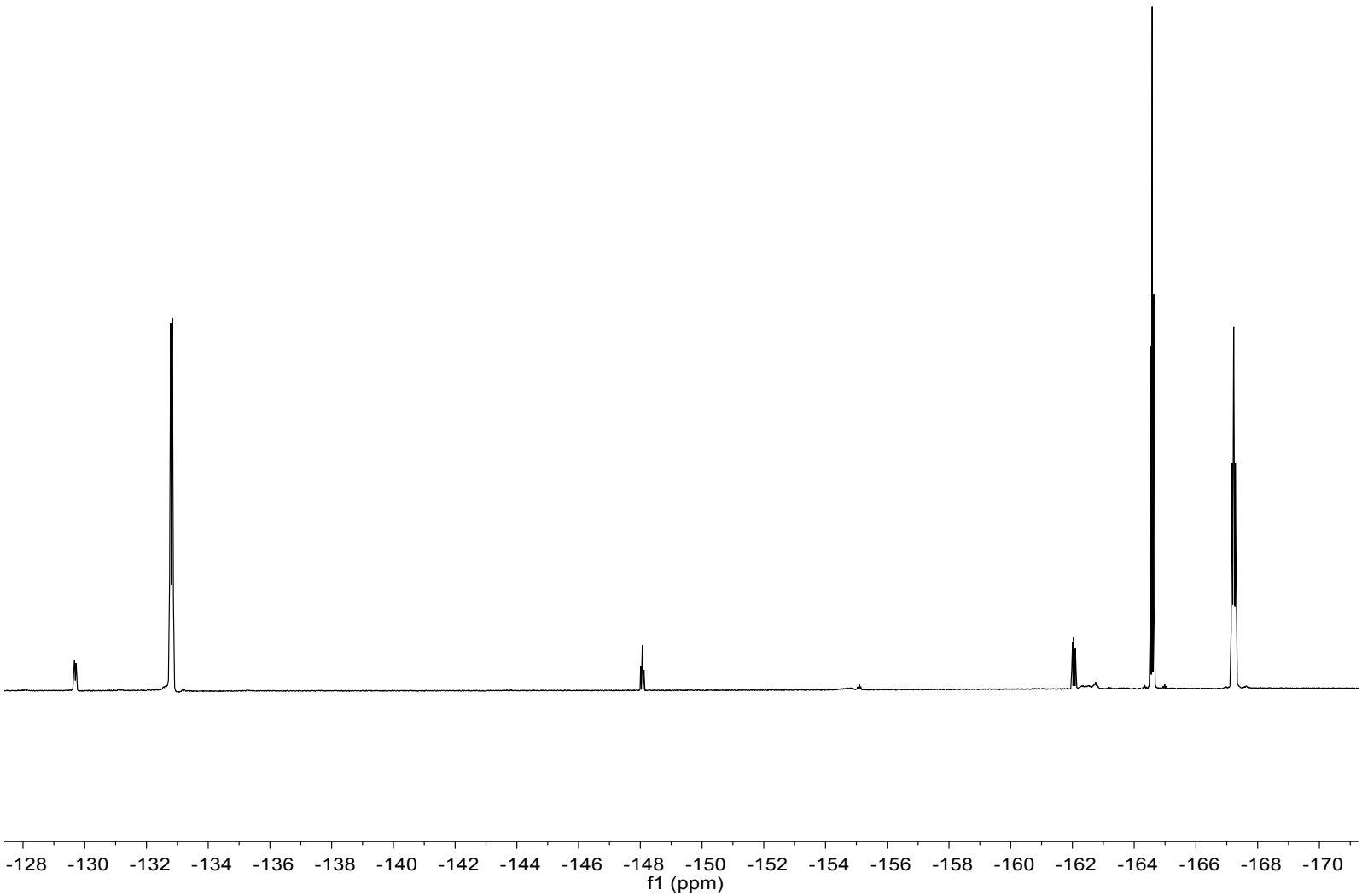

Figure S9. $^{19}F\{^{1}H\}$ NMR spectrum (376 MHz, CD_2Cl_2, 298 K) of **[2b]$^+$[MeB(C_6F_5)$_3$]$^-$**.

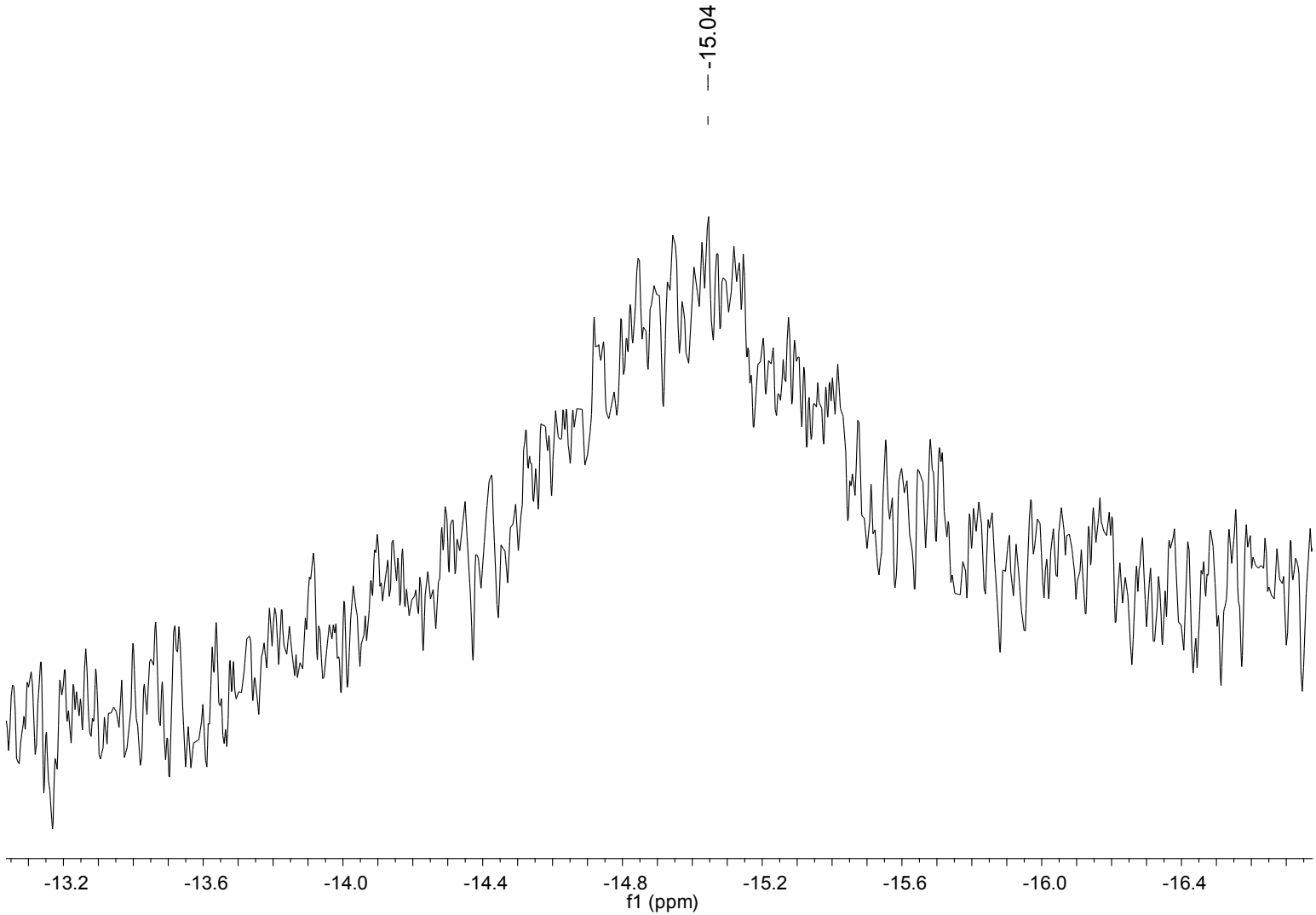

Figure S10. $^{11}B\{^{1}H\}$ NMR spectrum (128 MHz, CD_2Cl_2, 298 K) of **[2b]$^+$[MeB(C_6F_5)$_3$]$^-$**.

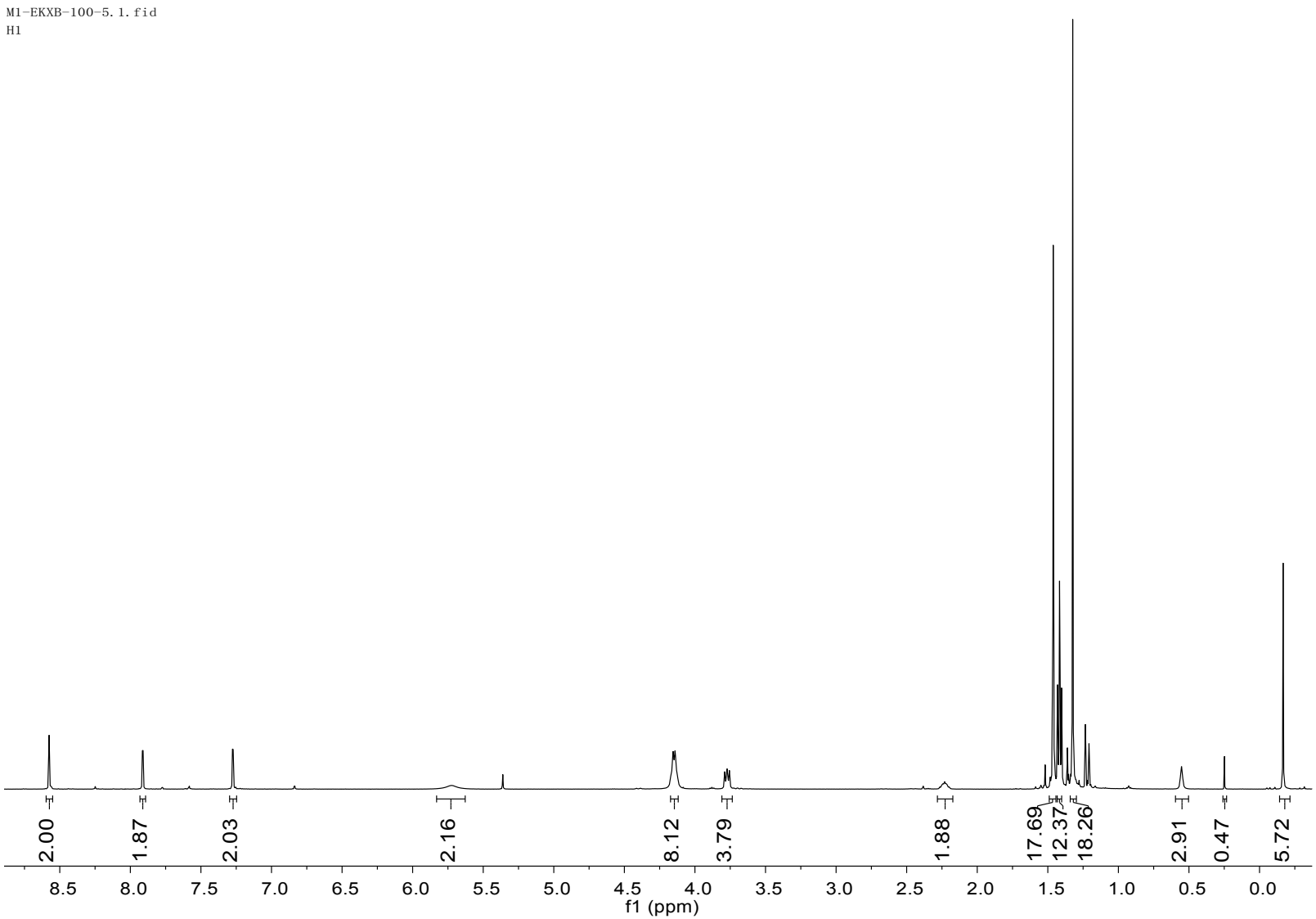

Figure S11. ^{1}H NMR spectrum (500 MHz, CD_2Cl_2, 298 K) of $[\mathbf{3a}\cdot(OEt_2)_2]^{2+}[(Me)B(C_6F_5)_3]^{-}[H_2N\{B(C_6F_5)_3\}_2]^{-}$.

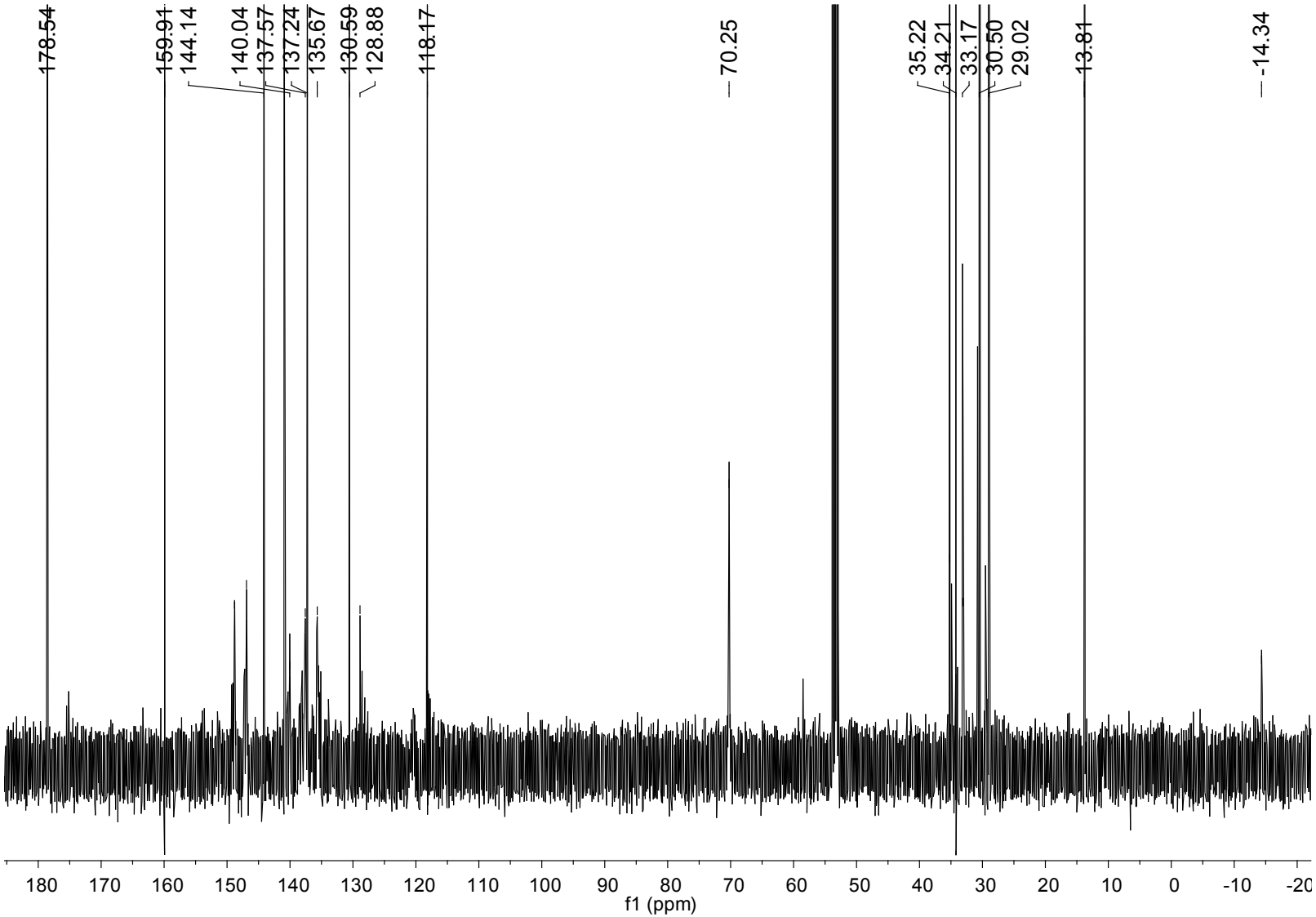

Figure S12. $^{13}C\{^{1}H\}$ NMR spectrum (125 MHz, CD_2Cl_2, 298 K) of $[\mathbf{3a}\cdot(\mathbf{OEt_2})_2]^{2+}[(\mathbf{Me})\mathbf{B}(\mathbf{C_6F_5})_3]^{-}[\mathbf{H_2N}\{\mathbf{B}(\mathbf{C_6F_5})_3\}_2]^{-}$.

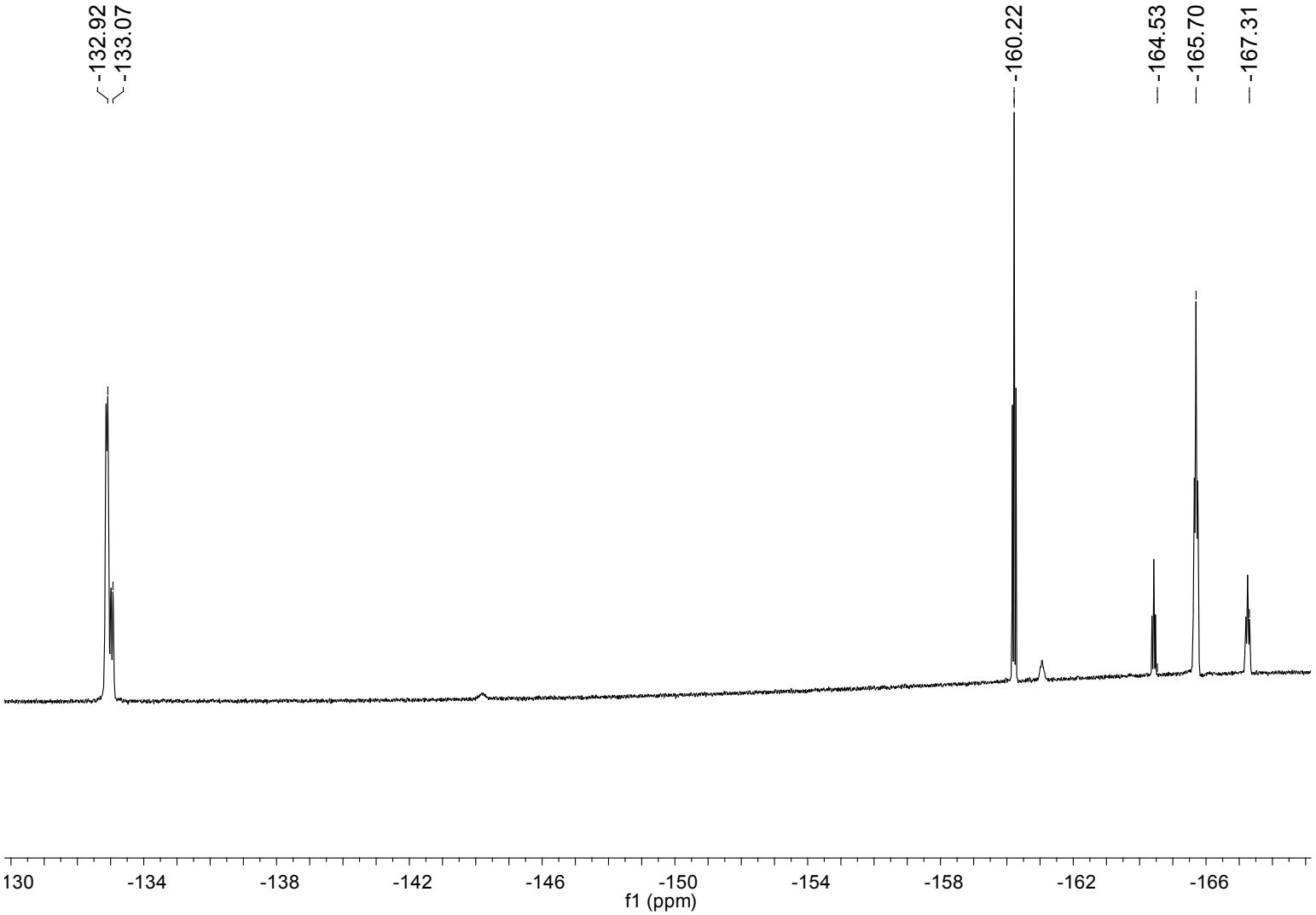

Figure S13. $^{19}F\{^{1}H\}$ NMR spectrum (376 MHz, CD_2Cl_2, 298 K) of $[\mathbf{3a}\cdot(\mathbf{OEt_2})_2]^{2+}[(\mathbf{Me})\mathbf{B}(\mathbf{C_6F_5})_3]^{-}[\mathbf{H_2N}\{\mathbf{B}(\mathbf{C_6F_5})_3\}_2]^{-}$.

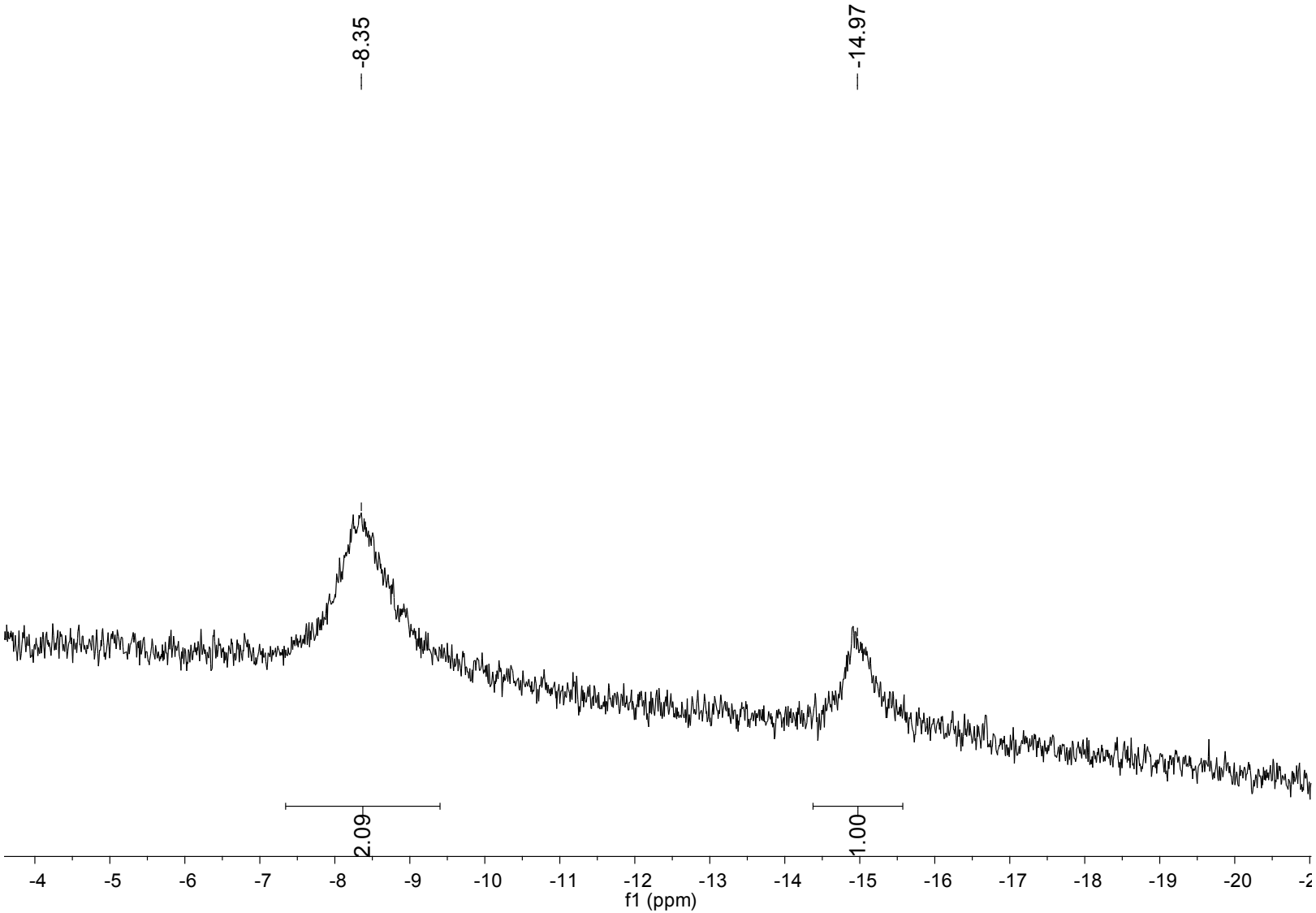

Figure S14. $^{11}B\{^{1}H\}$ NMR spectrum (128 MHz, CD_2Cl_2, 298 K) of $[\mathbf{3a{\cdot}(OEt_2)_2}]^{2+}[\mathbf{(Me)B(C_6F_5)_3}]^{-}[\mathbf{H_2N\{B(C_6F_5)_3\}_2}]^{-}$.

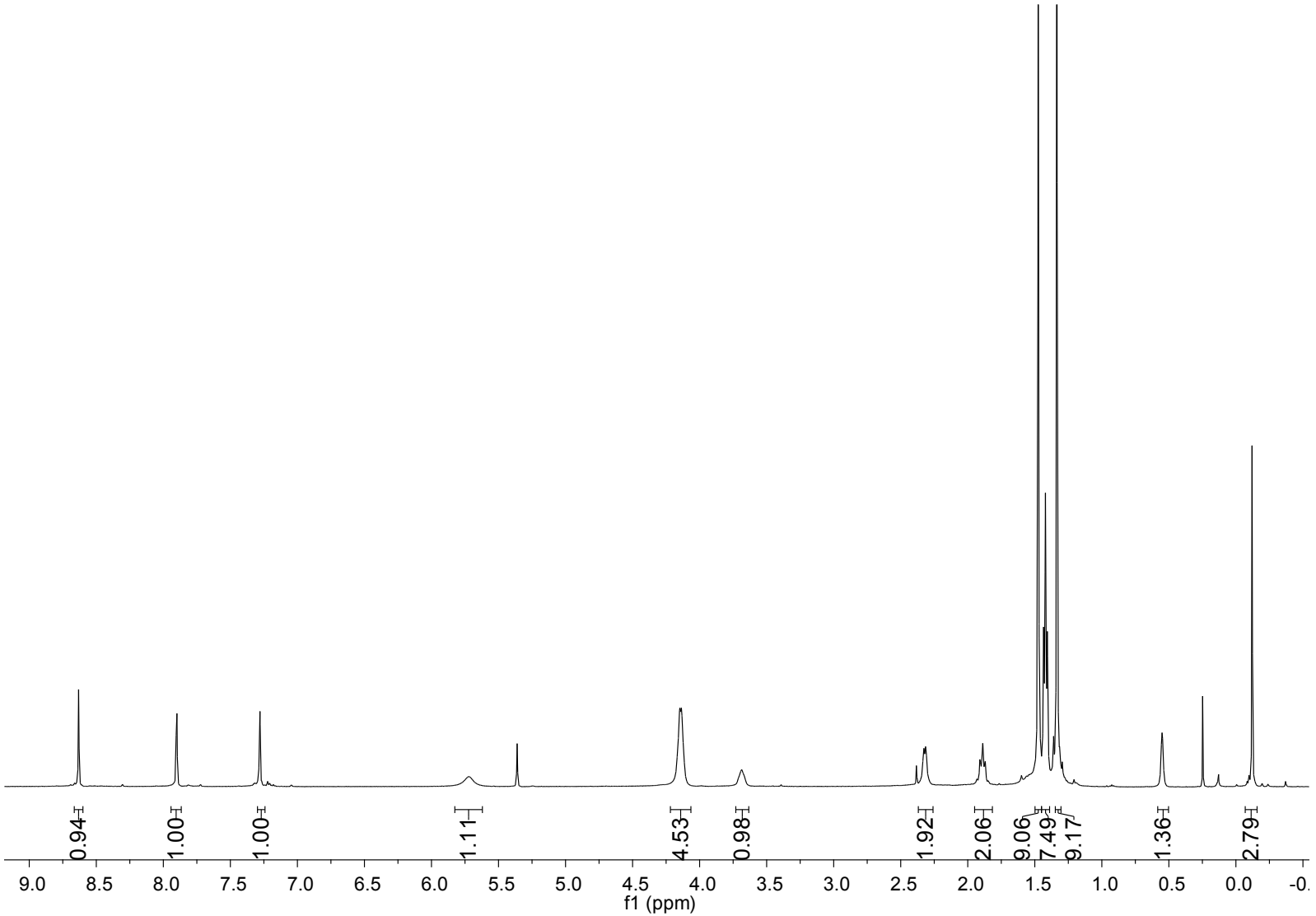

Figure S15. ^{1}H NMR spectrum (500 MHz, CD_2Cl_2, 298 K) of $[\mathbf{3b}\cdot(OEt_2)_2]^{2+}[(Me)B(C_6F_5)_3]^{-}[H_2N\{B(C_6F_5)_3\}_2]^{-}$.

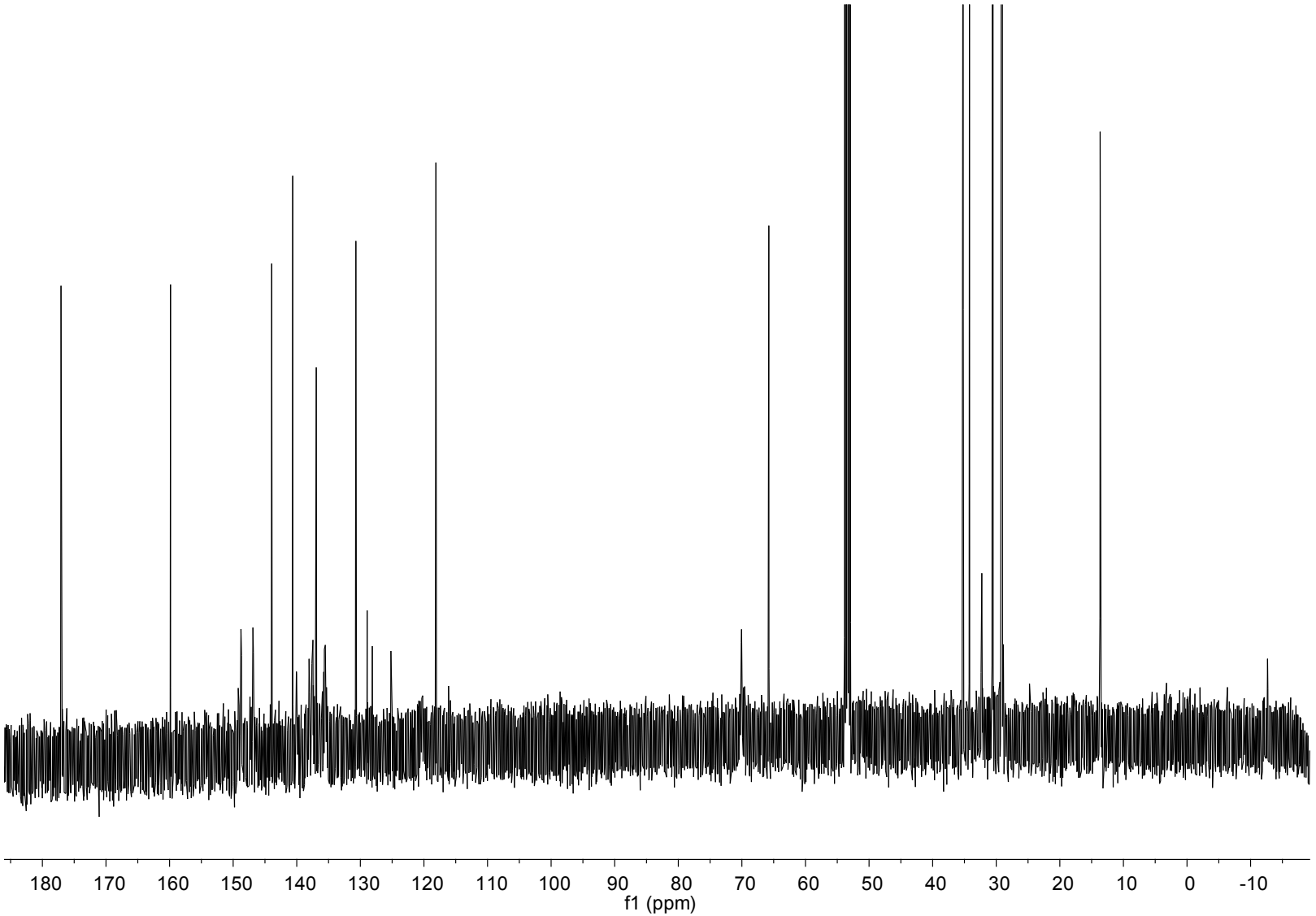

Figure S16. ^{13}C NMR spectrum (125 MHz, CD_2Cl_2, 298 K) of $[\mathbf{3b{\cdot}(OEt_2)_2}]^{2+}[\mathbf{(Me)B(C_6F_5)_3}]^{-}[\mathbf{H_2N\{B(C_6F_5)_3\}_2}]^{-}$.

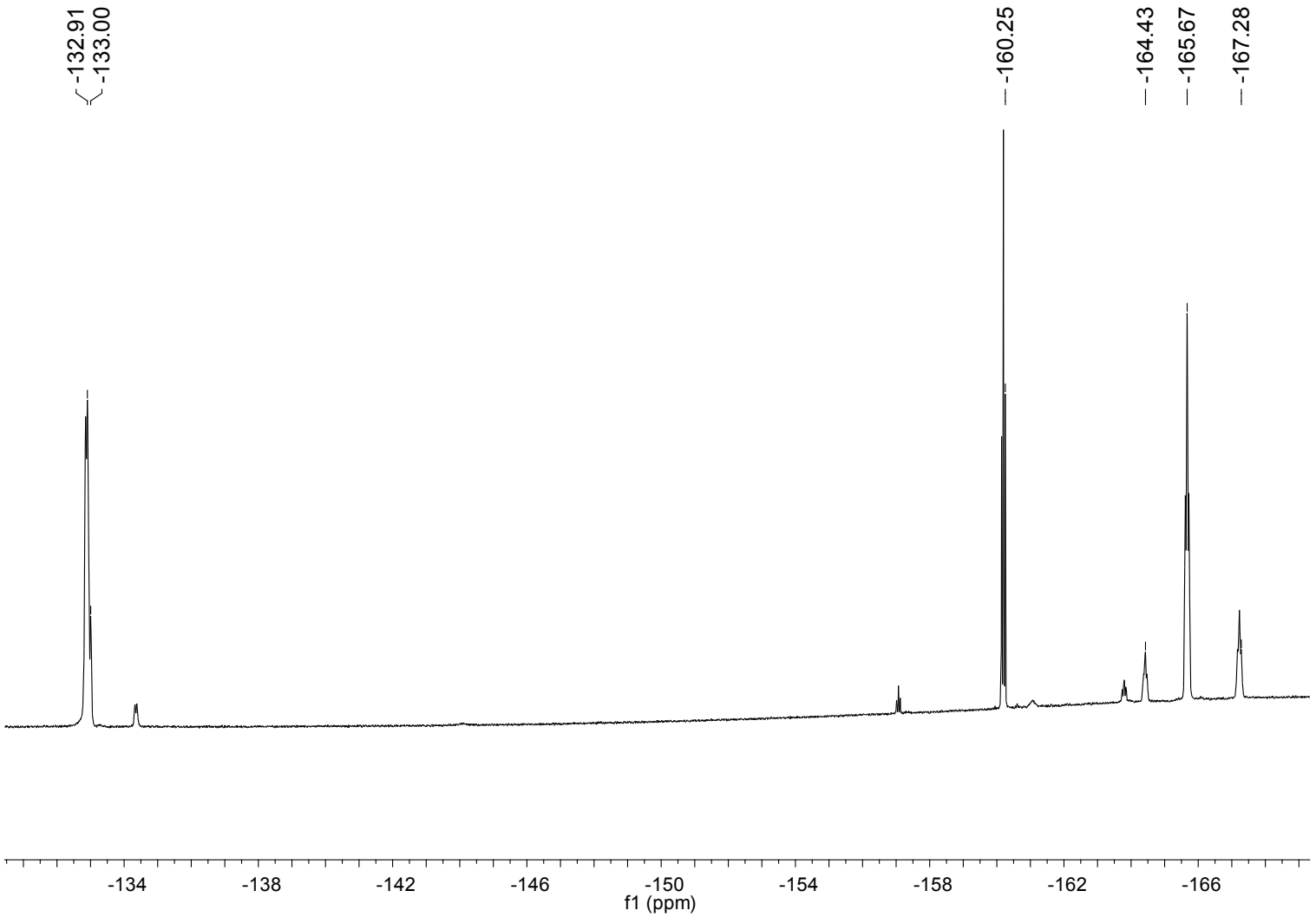

Figure S17. $^{19}F\{^{1}H\}$ NMR spectrum (376 MHz, CD_2Cl_2, 298 K) of $[\mathbf{3b}\cdot(\mathbf{OEt_2})_2]^{2+}[(\mathbf{Me})\mathbf{B}(\mathbf{C_6F_5})_3]^{-}[\mathbf{H_2N}\{\mathbf{B}(\mathbf{C_6F_5})_3\}_2]^{-}$.

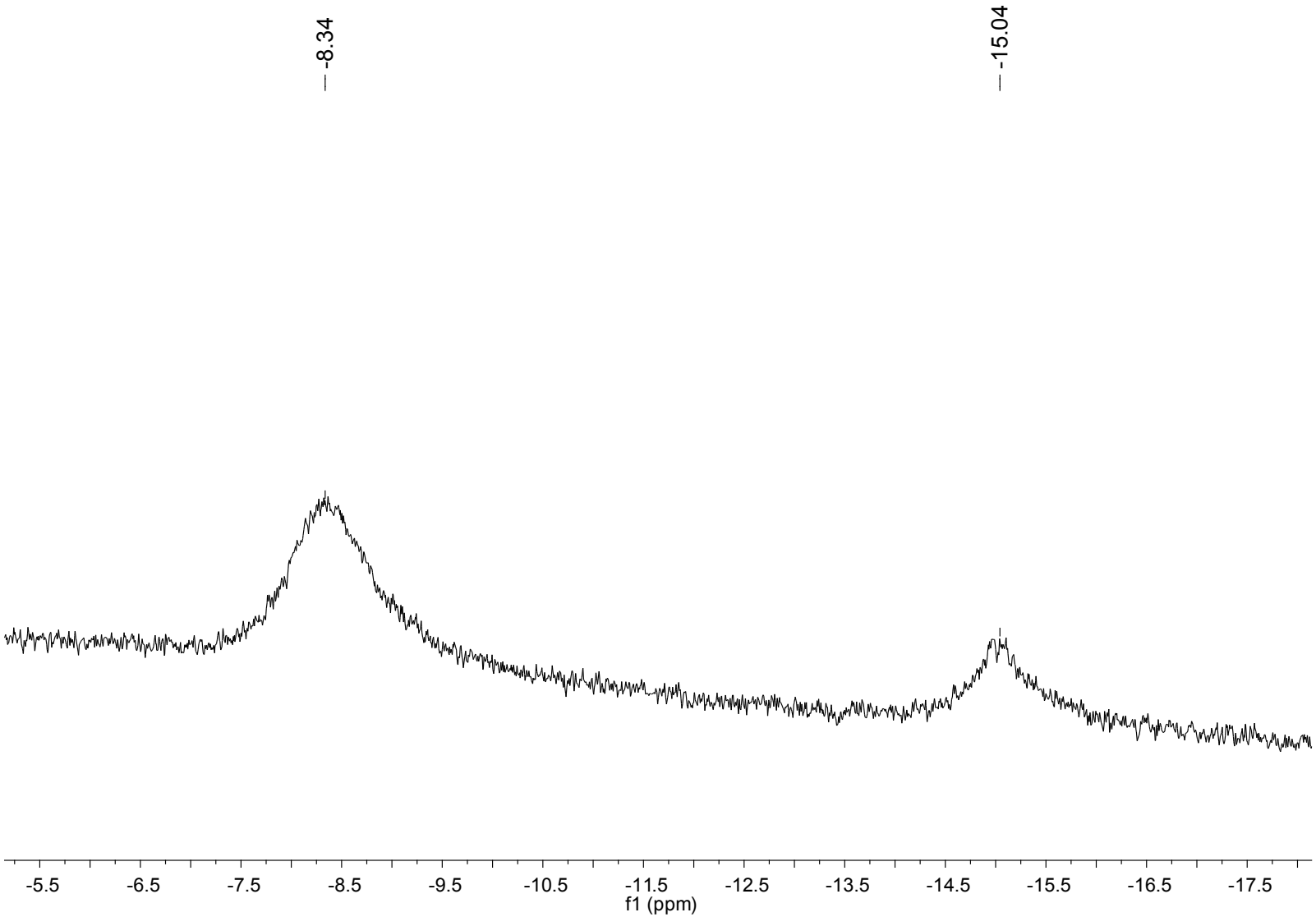

Figure S18. $^{11}B\{^{1}H\}$ NMR spectrum (128 MHz, CD_2Cl_2, 298 K) of $[\mathbf{3b{\cdot}(OEt_2)_2}]^{2+}[\mathbf{(Me)B(C_6F_5)_3}]^{-}[\mathbf{H_2N\{B(C_6F_5)_3\}_2}]^{-}$.

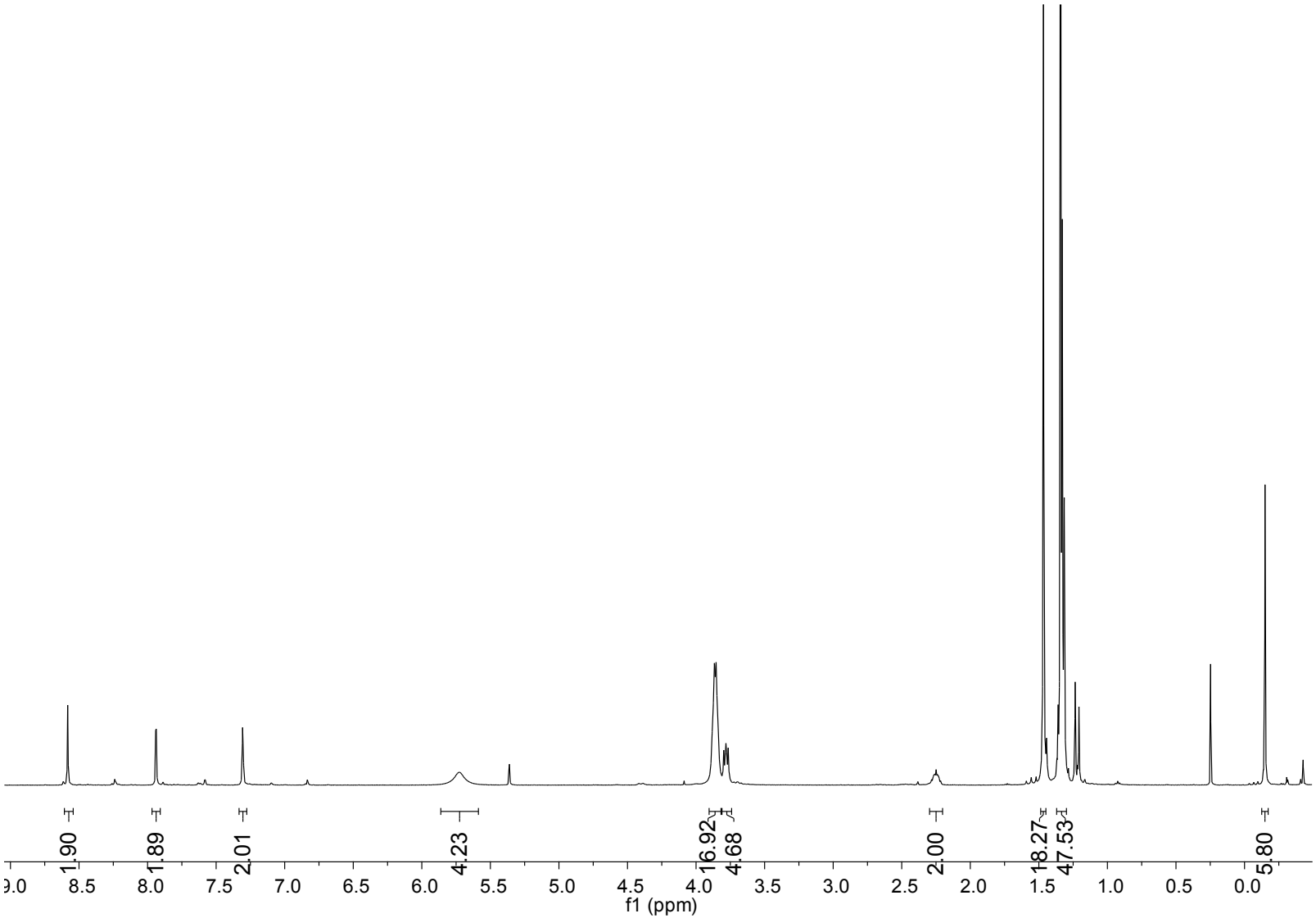

Figure S19. ^{1}H NMR spectrum (500 MHz, CD_2Cl_2, 298 K) of **[3a·(OEt$_2$)$_2$]$^{2+}$[H$_2$N{B(C$_6$F$_5$)$_3$}$_2$]$^{-}$$_2$**.

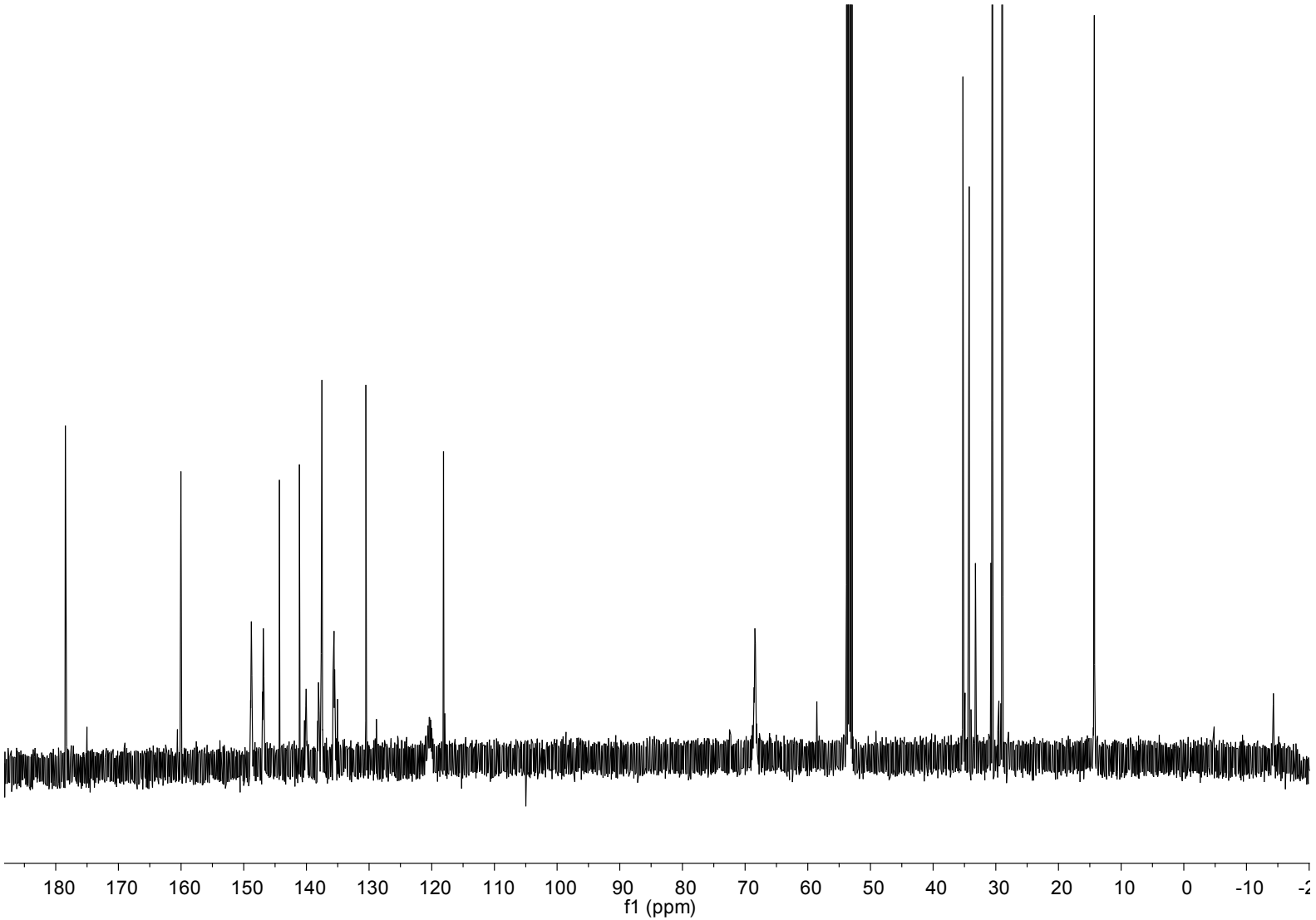

Figure S20. $^{13}C\{^{1}H\}$ NMR spectrum (125 MHz, CD_2Cl_2, 298 K) of **[3a·(OEt$_2$)$_2$]$^{2+}$[H$_2$N{B(C$_6$F$_5$)$_3$}$_2$]$^{-}_2$**.

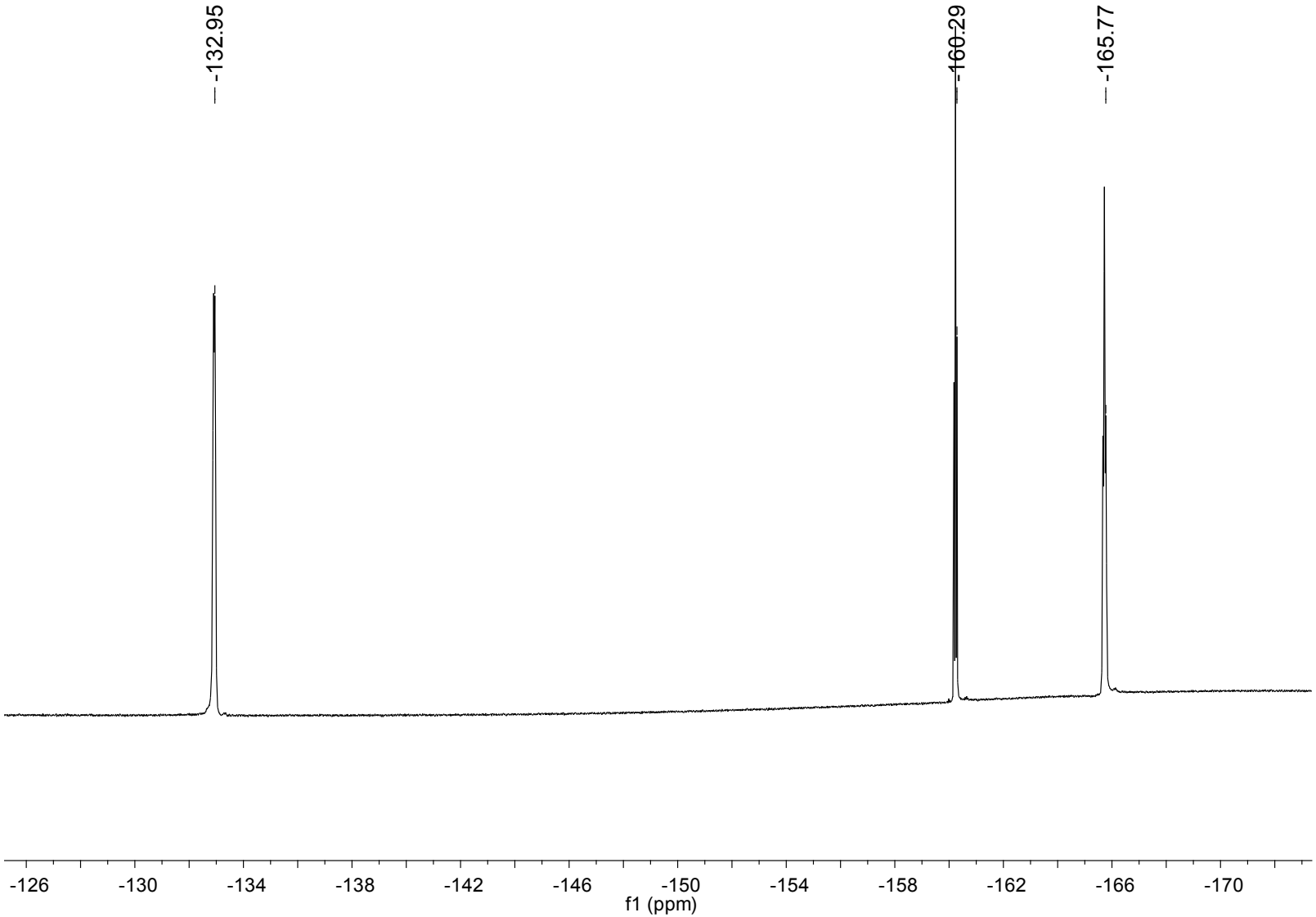

Figure S21. $^{19}F\{^{1}H\}$ NMR spectrum (376 MHz, CD_2Cl_2, 298 K) of **[3a·(OEt$_2$)$_2$]$^{2+}$[H$_2$N{B(C$_6$F$_5$)$_3$}$_2$]$^{-}$$_2$**.

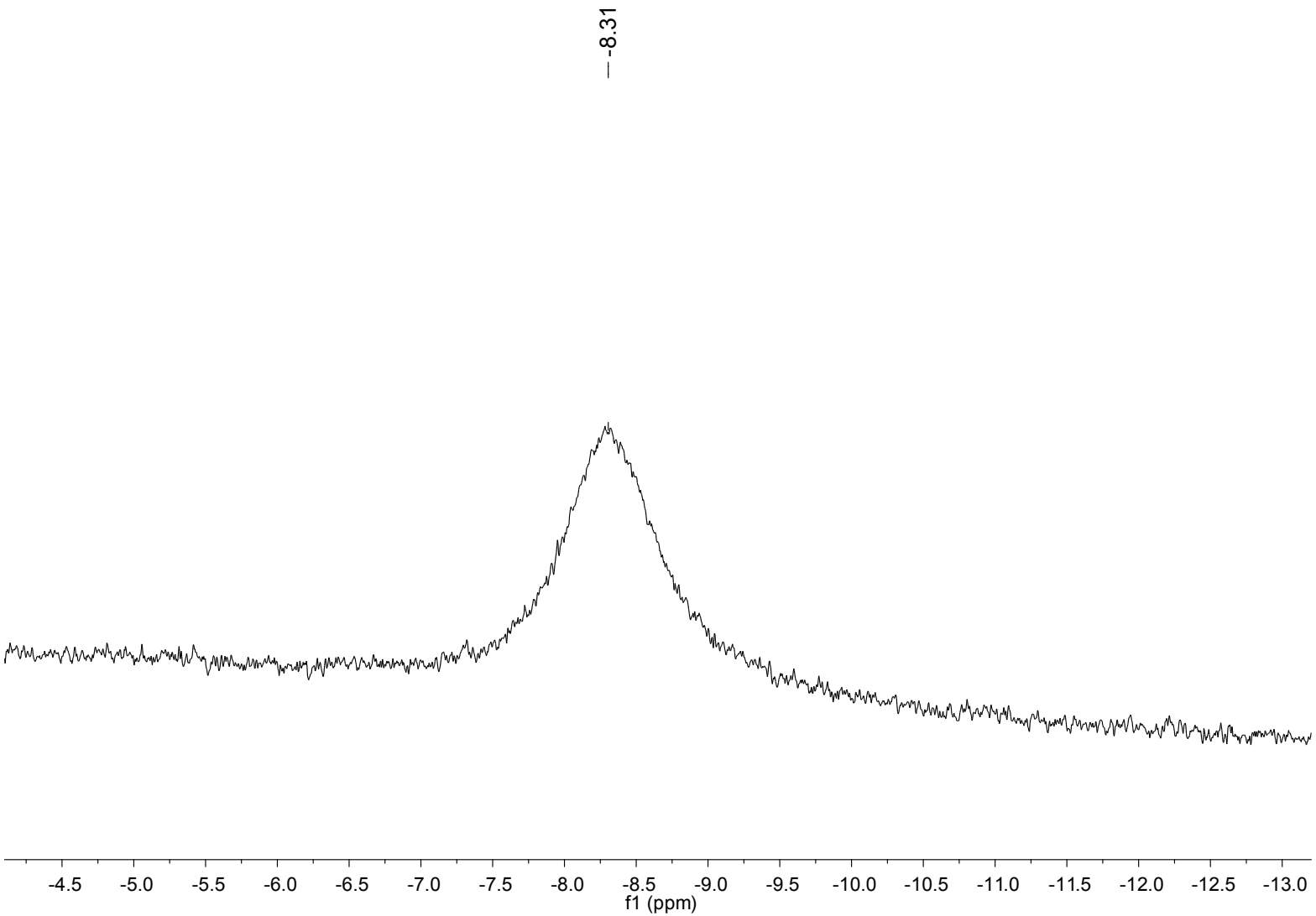

Figure S22. $^{11}B\{^{1}H\}$ NMR spectrum (128 MHz, CD_2Cl_2, 298 K) of **[3a·(OEt$_2$)$_2$]$^{2+}$[H$_2$N{B(C$_6$F$_5$)$_3$}$_2$]$^{-}$$_2$**.

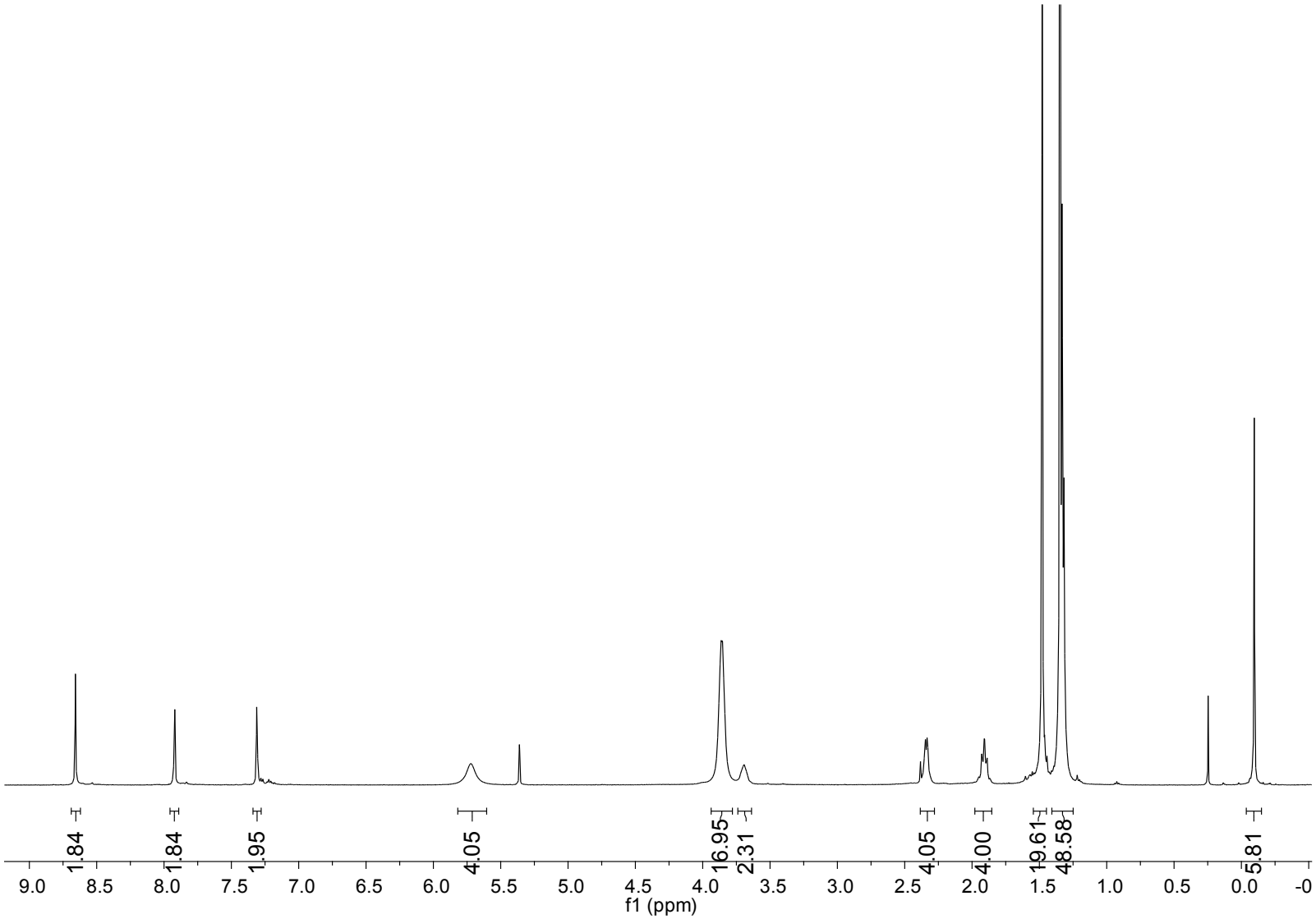

Figure S23. ^{1}H NMR spectrum (500 MHz, CD_2Cl_2, 298 K) of $\mathbf{[3b{\cdot}(OEt_2)_2]^{2+}[H_2N\{B(C_6F_5)_3\}_2]^{-}{}_2}$.

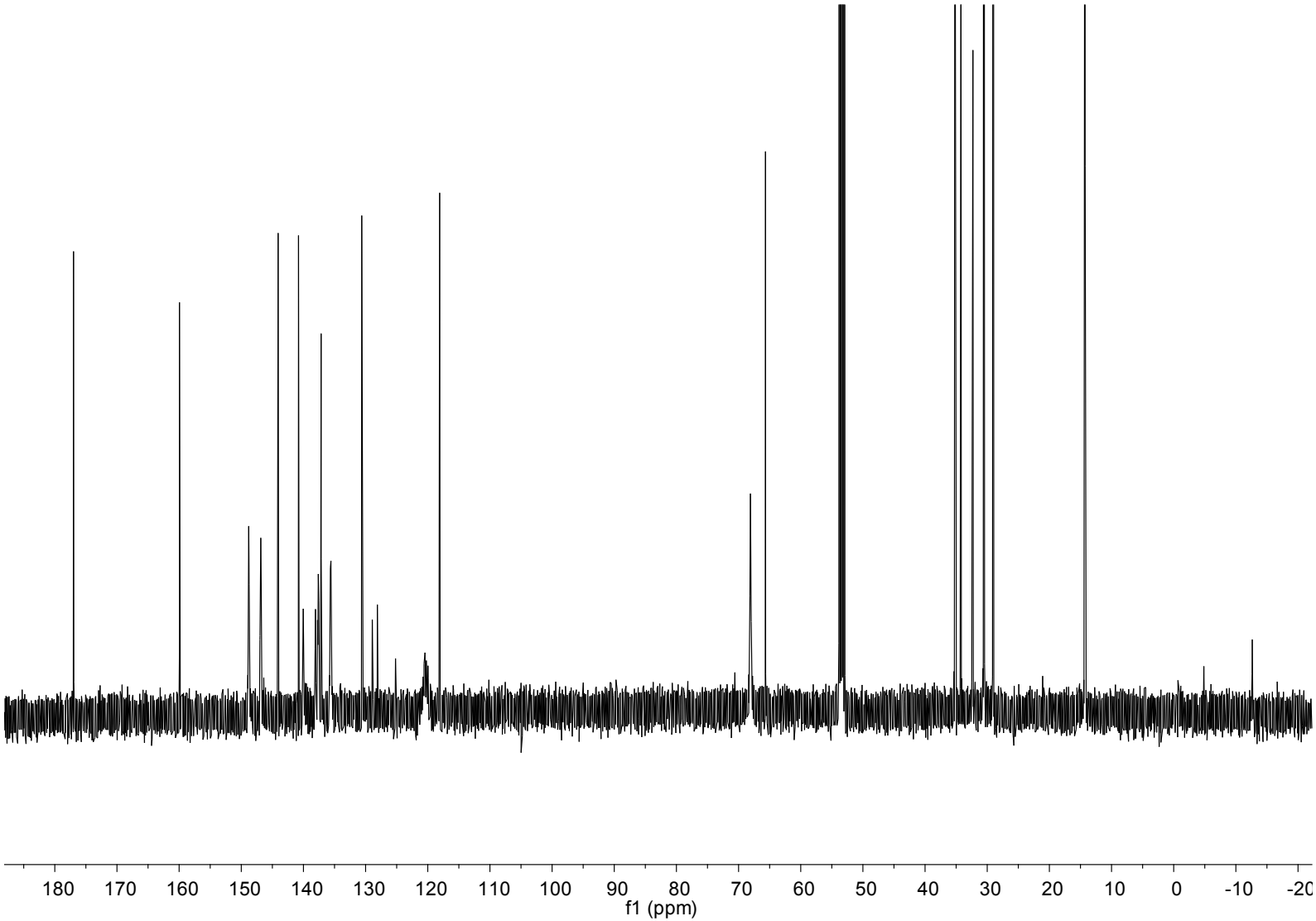

Figure S24. $^{13}C\{^{1}H\}$ NMR spectrum (125 MHz, CD_2Cl_2, 298 K) of $\mathbf{[3b{\cdot}(OEt_2)_2]^{2+}[H_2N\{B(C_6F_5)_3\}_2]^-_2}$.

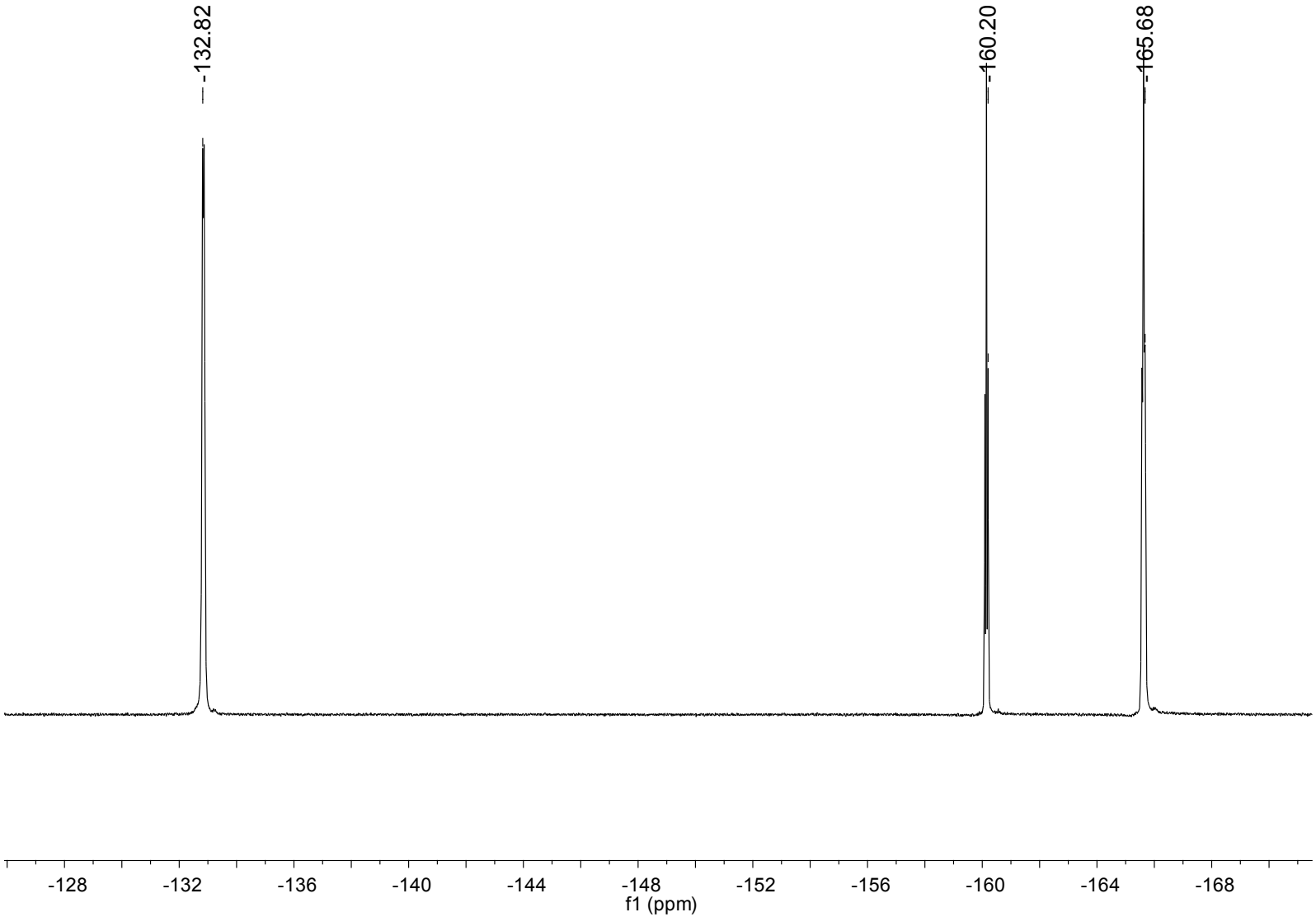

Figure S25. $^{19}F\{^{1}H\}$ NMR spectrum (376 MHz, CD_2Cl_2, 298 K) of **[3b·(OEt$_2$)$_2$]$^{2+}$[H$_2$N{B(C$_6$F$_5$)$_3$}$_2$]$^{-}_2$**.

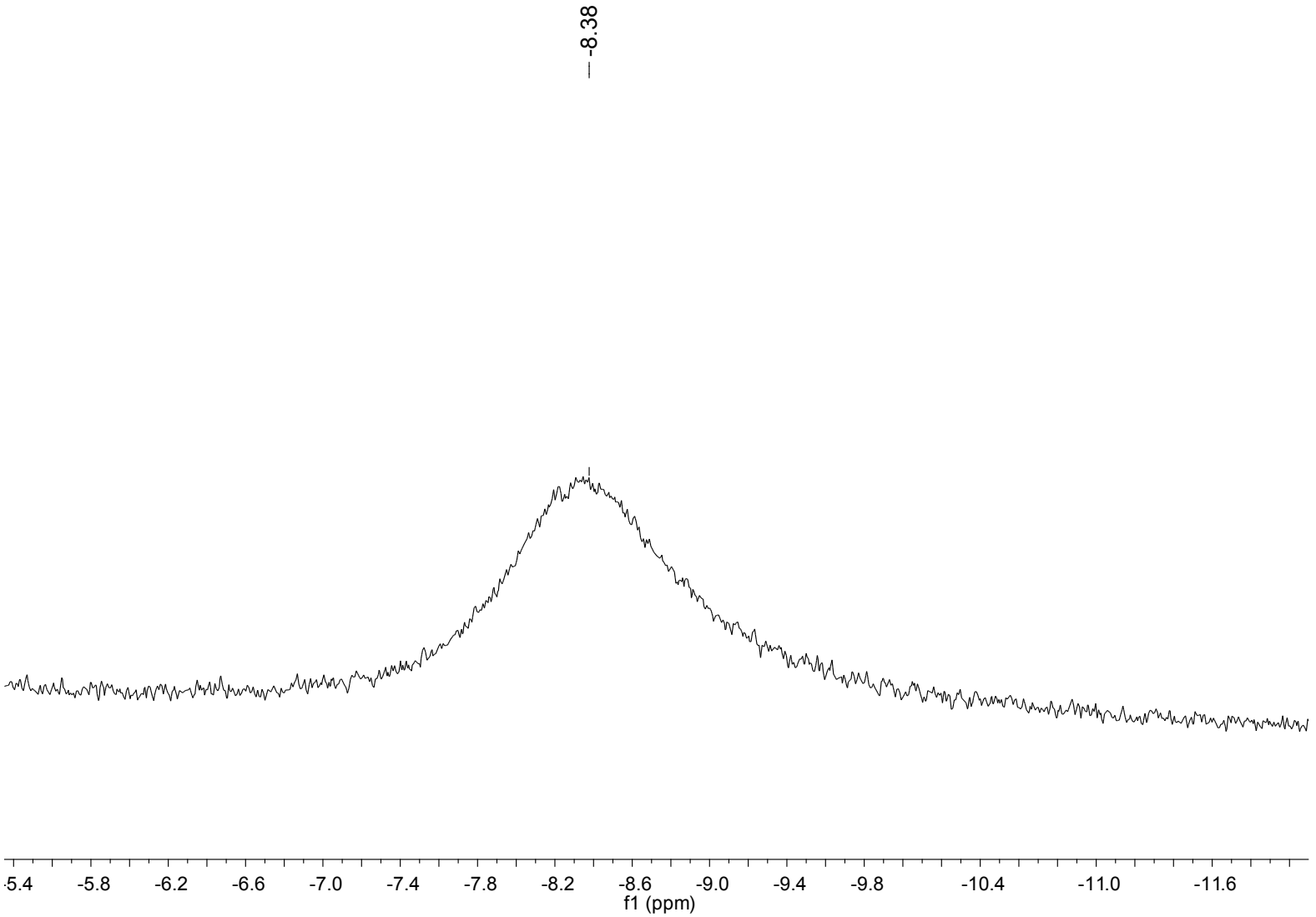

Figure S26. $^{11}B\{^{1}H\}$ NMR spectrum (128 MHz, CD_2Cl_2, 298 K) of **[3b·(OEt$_2$)$_2$]$^{2+}$[H$_2$N{B(C$_6$F$_5$)$_3$}$_2$]$^{-}_2$**.

Table S1. Summary of Crystal and Refinement Data for Complexes **4a** and **[3b·(OEt$_2$)$_2$]$^{2+}$[H$_2$N{B(C$_6$F$_5$)$_3$}$_2$]$^-_2$**.

	4a	**[3b·(OEt$_2$)$_2$]$^{2+}$[H$_2$N{B(C$_6$F$_5$)$_3$}$_2$]$^-_2$**
Empirical formula	$C_{39}H_{48}AlF_5N_2O_2$	$C_{81.33}H_{60}Al_{1.33}B_{2.67}Cl_{5.33}F_{40}N_{2.67}O_{2.67}$
Formula weight	698.77	2131.18
Crystal system	monoclinic	monoclinic
Space group	C 2 / c	P 1 2_1 / c 1
a, Å	37.742(7)	21.0007(15)
b, Å	10.4163(19)	19.4971(14)
c, Å	21.203(3)	19.4648(17)
α, deg	90	90
β, deg	106.565(7)	113.882(4)
γ, deg	90	90
Volume, Å^3	7990(2)	7287.5(10)
Z	8	3
Density, g.m^{-3}	1.162	1.457
Abs. coeff., mm^{-1}	0.107	0.293
F(000)	2960	3208
Crystal size, mm	0.36 x 0.26 x 0.13	0.580 x 0.410 x 0.200
θ range, deg	2.94 to 27.48	2.955 to 27.424
Limiting indices	$-48 \le h \le 48$, $-11 \le k \le 13$, $-27 \le l \le 24$	$-23 \le h \le 27$, $-25 \le h \le 24$, $-25 \le h \le 25$
Reflec. Collected	26825	38629
Refle. Unique [I > 2*σ*(I)]	9058	16588
Data/restrains/param.	9058 / 15 / 455	16588 / 4 / 881
Goodness-of-it on F^2	0.763	0.965
R_1 [I > 2*σ*(I)] (all data)	0.0797	0.1298
wR_2 [I > 2*σ*(I)] (all data)	0.1918	0.3422
Largest diff. e.A^{-3}	0.344 and –0.287	1.859 and –1.115